Psychiatry Research: Neuroimaging 345 (2024) 111891

Contents lists available at ScienceDirect

Psychiatry Research: Neuroimaging

journal homepage: www.elsevier.com/locate/psychresns

Characterization of neural networks involved in transdiagnostic emotion dysregulation from a pilot randomized controlled trial of a neurostimulation-enhanced behavioral intervention

Andrada D. Neacsiu [a,b,1,*], Nimesha Gerlus [c,1], John L. Graner [c], Lysianne Beynel [a,d], Moria J. Smoski [a,c], Kevin S. LaBar [a,c]

[a] Department of Psychiatry and Behavioral Sciences, Duke University, Durham, NC, USA
[b] Brain Stimulation Research Center, Duke University, Durham, NC, USA
[c] Department of Psychology, Duke University, Durham, NC, USA
[d] National Institute of Mental Health, Experimental Therapeutics and Pathophysiology Branch, Noninvasive Neuromodulation Unit, Bethesda, MD, USA

ARTICLE INFO

Keywords:
Prefrontal cortex
Transdiagnostic
Emotional dysregulation
FMRI
RTMS

ABSTRACT

Background: Emotional dysregulation is a serious and impairing mental health problem. We examined functional activity and connectivity of neural networks involved in emotional dysregulation at baseline and following a pilot neurostimulation-enhanced cognitive restructuring intervention in a transdiagnostic clinical adult sample.
Methods: Neuroimaging data were analyzed from adults who scored 89 or higher on the Difficulties with Emotion Regulation (DERS) scale and had at least one DSM-5 diagnosis. These participants were part of a pilot randomized, double-blind, placebo-controlled trial combining a single therapeutic session of cognitive restructuring with active or sham transcranial magnetic stimulation over the dorsolateral prefrontal cortex. During the study, participants engaged in an emotional regulation task using personalized autobiographical stressors while undergoing functional magnetic resonance imaging (fMRI) before and after the pilot intervention. The fMRI task required participants to either experience the emotions associated with the memories or apply cognitive restructuring strategies to reduce their distress.
Results: Whole-brain fMRI results during regulation at baseline revealed increased activation in the dorsal frontoparietal network but decreased activation in the supplementary motor area, cingulate cortex, insula, and ventrolateral prefrontal cortex (vlPFC). Emotion dysregulation was associated with greater vmPFC and amygdala activation and functional connectivity between these regions. The strength of functional connectivity between the dlPFC and other frontal regions was also a marker of emotional dysregulation. Preliminary findings from a subset of participants who completed the follow-up fMRI scan showed that active neurostimulation improved behavioral indices of emotion regulation more than sham stimulation. A whole-brain generalized psychophysiological interaction analysis indicated that active neurostimulation selectively increased occipital cortex connectivity with both the insula and the dlPFC. Region-of-interest functional connectivity analyses showed that active neurostimulation selectively increased dlPFC connectivity with the insula and orbitofrontal cortex (OFC).
Conclusion: Insufficient neural specificity during the emotion regulation process and over-involvement of frontal regions may be a marker of emotional dysregulation across disorders. OFC, vlPFC, insula activity, and connectivity are associated with improved emotion regulation in transdiagnostic adults. In this pilot study, active neurostimulation led to neural changes in the emotion regulation network after a single session; however, the intervention findings are preliminary, given the small sample size. These functional network properties can inform future neuroscience-driven interventions and larger-scale studies.

* Corresponding author.
E-mail address: andrada.neacsiu@duke.edu (A.D. Neacsiu).
[1] Equal contributions

https://doi.org/10.1016/j.pscychresns.2024.111891
Received 30 April 2024; Received in revised form 30 August 2024; Accepted 3 September 2024
Available online 5 September 2024

1. Characterization of neural networks involved in transdiagnostic emotional dysregulation

Emotional dysregulation, characterized by difficulties effectively reducing emotional arousal, profoundly impacts mental health and overall well-being. The neuroscience of cognitively mediated emotional regulation has been extensively examined in non-clinical samples (Gross, 2015). These studies have found activation distributed throughout a fronto-limbic network, including the dorsolateral prefrontal cortex (dlPFC), ventrolateral PFC (vlPFC), dorsomedial prefrontal cortex (dmPFC), frontal pole, amygdala, and insula (Powers and LaBar, 2019; Ochsner et al., 2012; Pico-Perez et al., 2017) as well as the medial prefrontal (mPFC) and orbitofrontal cortex (OFC) (Goldin et al., 2008; Dörfel et al., 2014; Suzuki and Tanaka, 2021). Taken together, these findings suggest that increased engagement of regulatory processes is indicated by increased activity in the PFC, which then reduces subcortical, limbic, and paralimbic activity (i.e., amygdala and insula) associated with emotional reactivity (Etkin et al., 2015). Of the PFC subregions involved in regulation, the lateral PFC preferentially appraises emotional states and goal-related regulation strategies, whereas the OFC and mPFC appraise external sensory stimuli, episodic memories, and imagined events, as well as the mental state of self and others (Dixon et al., 2017).

Disruptions in this circuitry have been associated with difficulties in emotion regulation in clinical samples. Across mood and anxiety disorders, hypoactivation in PFC regions [e.g., dlPFC, vlPFC, dmPFC (Pico-Perez et al., 2017; Zilverstand et al., 2017)] and hyperactivation in limbic/paralimbic brain areas [e.g., left anterior insula (Pico-Perez et al., 2017)], characterize difficulties in changing emotional arousal. Furthermore, hyperactivation in the ventromedial PFC (vmPFC) during emotion regulation has also been found in depressed compared to non-depressed samples (Stephanou et al., 2017). In subcortical regions, hyperactivity in the amygdala and hypoactivity in the anterior cingulate cortex (ACC) and inferior/superior parietal cortex differentiate clinical adults from non-clinical controls but tend to indicate disorder-specific impairments with emotion regulation (Zilverstand et al., 2017). These findings provide a rigorous scientific foundation for alterations in the emotion regulation circuitry that cut across clinical disorders (Fernandez et al., 2016). Nevertheless, most studies were conducted within a specific disorder (e.g., major depressive disorder only), not transdiagnostically, and studies examining longitudinal changes in emotional dysregulation across disorders are lacking.

Based on the modal model of emotion generation, emotions occur based on the sequential occurrences of a situation, attentional allocation, appraisal, and response (Gross, 2013). This process model proposes that five strategies comprise emotion regulation; one of these five strategies is cognitive change or emotion reappraisal. Reappraisal attempts to modify an emotional response by changing the significance attributed to the emotional event. Cognitive restructuring (CR) is a clinical intervention in which reappraisal is targeted as a change mechanism in treating psychopathology (Clark, 2013; Neacsiu et al., 2013). CR is a fundamental cognitive emotion regulation skill taught in most evidence-based psychotherapies (Hawley et al., 2017; Goldin et al., 2012; Kaczkurkin and Foa, 2015) that has been extensively studied in basic neuroscience (Powers and LaBar, 2019; Ochsner et al., 2012; Webb et al., 2012). CR involves thinking differently about a situation to change the emotional experience, which can be achieved via several tactics, such as reframing and distancing (Powers and LaBar, 2019; Pico-Perez et al., 2017). Noninvasive neurostimulation, such as repetitive transcranial magnetic stimulation (rTMS), has been shown to enhance the use of CR in altering emotional processes in both healthy (Feeser et al., 2014) and clinical (Neacsiu et al., 2021) samples, especially if brain activity is directed during stimulation (Luber et al., 2017).

To examine regulation mechanisms in the brain, emotional stimuli are typically used to induce affect. Typical emotional stimuli used in emotional induction paradigms include images, movie clips, audio clips, and autobiographical recall. Autobiographical memories have been shown to induce affect reliably (Mills and D'Mello, 2014; Holland and Kensinger, 2010), and have the added advantage of personal relevance to participants compared to standardized visual or auditory stimuli. They also offer ecological validity in that they are the closest approximation in the lab to what happens in a psychotherapy session. In healthy controls, studies of cognitive appraisal to downregulate negative affect induced by autobiographical memory recall show neural changes in cognitive control regions, such as the PFC, as well as in emotion generation regions, such as the insula and amygdala (Holland and Kensinger, 2013; Kross et al., 2009). Clinical studies of cognitive reappraisal also implicate regions comprising the frontoparietal network during regulation (Pico-Perez et al., 2017; De la Peña-Arteaga et al., 2021; Keller et al., 2022). One clinical study that used autobiographical memory recall combined with reappraisal showed elevated amygdala activity and greater amygdala-hippocampal connectivity to unregulated memories in major depressive disorder and a unique downregulation profile in the posterior hippocampus relative to healthy controls (Doré et al., 2018).

This manuscript reports on a follow-up analysis of a previously published pre-registered (NCT02573246), double-blinded, placebo-controlled trial (Neacsiu et al., 2021; Neacsiu et al., 2022) of a one-time transdiagnostic intervention for emotional dysregulation. Transdiagnostic participants were randomized to receive a single session of CR practice augmented with either active or sham rTMS targeted towards a dlPFC node in the emotion regulation neural network to enhance skill acquisition and use. In the parent trial, active neurostimulation led to significant improvements in psychophysiological emotion regulation and lower regulation duration during the intervention when compared to sham. Furthermore, receiving active versus sham rTMS increased the likelihood of using CR during the week following the intervention.

In this paper, we report on findings from the neuroimaging scans taken before and after this intervention (Neacsiu et al., 2022) when participants used autobiographical memory cues to induce negative affect and subsequently downregulated distress associated with these memories. These analyses serve two main aims. The first aim is to characterize the brain circuitry associated with emotional regulation and dysregulation in a transdiagnostic sample, focusing on activation patterns at baseline. We expected significant changes in functional activity during emotion regulation in the amygdala, insula, dlPFC, dmPFC, vlPFC, vmPFC, and OFC. We hypothesized that self-reported difficulties with emotion regulation would negatively correlate with activation in these prefrontal regions and positively correlate with amygdala and insula activations (Hypothesis 1a). We also hypothesized that dlPFC-amygdala functional connectivity would be significant during regulation and correlate with effective emotion regulation (Hypothesis 1b). Connectivity between limbic (amygdala, insula) and prefrontal regions involved in regulation (dlPFC, vlPFC, vmPFC, dmPFC, OFC) were also explored in relation to behavioral regulation and dysregulation. Furthermore, connectivity between the dlPFC (the target of neurostimulation) and other prefrontal regions and correlations with emotional regulation and dysregulation were examined. Finally, we investigated how changes in neural activation and connectivity after the intervention correlated with changes in reported emotional regulation and dysregulation.

The second exploratory aim was to investigate the brain and behavioral effects of the pilot TMS-CR intervention. At the behavioral level, we expected that, compared to participants who received sham, participants who received active rTMS would evidence more decrease in distress after using CR in the MRI scanner (Hypothesis 2a) and higher activation in the prefrontal cortex (dlPFC, vlPFC, vmPFC, OFC) during emotion regulation (Hypothesis 2b). We also expected that the amygdala-dlPFC functional connectivity would increase more in the active versus sham condition (Hypothesis 2c). We explored whole-brain differential changes in activation and connectivity between conditions

and differences in connectivity between the amygdala, insula, and prefrontal ROIs. We also explored neural markers of intervention-related improvement in self-reported difficulties in emotion regulation in everyday living.

2. Materials and methods

2.1. Participant characteristics

Sample characteristics and trial design have been reported previously (Neacsiu et al., 2022) and are summarized here. Participants were between the ages of 18–65 years; met criteria for at least one DSM-5 disorder according to the Structured Clinical Interview (SCID-5) (First et al., 2015); were emotionally dysregulated as indicated by a score of 89 or higher on the Difficulties in Emotion Regulation Scale (DERS) (Gratz and Roemer, 2004); and were willing to participate in all aspects of the study. Participants were excluded if they endorsed current substance or alcohol abuse or a history of mania or psychosis; were currently in (or planning to start) CBT; needed immediate hospitalization; were at high risk for suicide; were at increased risk for seizure during neuromodulation; or met MRI exclusions. Pregnant persons, homeless adults, adults who could not travel to Duke, and who did not understand English or had low verbal IQ (Dunn, 1981) were also excluded. Participants were stratified to have different levels of proficiency with CR (low, medium, or high proficiency) using pre-established cutoffs on the emotion regulation questionnaire (ERQ) (Gross and John, 2003). The Duke University Health System Institutional Review Board approved the study. For a detailed diagram of participant flow through the enrollment, randomization, data collection, and analysis phases of the neurostimulation trial, see Fig. 1 in Ref. (Neacsiu et al., 2022).

A total of 36 participants completed the baseline MRI scan. One participant was excluded due to their inability to comply with the MRI instructions. Two participants were excluded due to excessive motion [3 or 4 runs with at least 20% of TRs above a framewise displacement threshold of 0.4 mm as in prior work done by our team (Powers et al., 2019) as well as others (Tozzi et al., 2024; Hu et al., 2024; Cooper et al., 2024; Power et al., 2012, 2014)]. Four participants had one or two fMRI baseline runs affected by extreme motion; these runs were excluded from the final analyses, but the participants were kept in with data from the remaining runs. We chose to exclude data using volume-wise motion censoring because this method provides statistical benefits for task-based fMRI analysis over a run-based exclusion criterion (Siegel et al., 2014; Jones et al., 2022). Therefore, baseline behavioral and MRI analyses examined 33 participants (M_{DERS} = 111.15, SD = 17.75). This set included six men and 27 women, ages 18 to 62, M = 34.15, SD = 13.74. See Table 1 for sample characteristics. Five participants discontinued before the TMS session, and three additional participants discontinued before the second MRI session. A total of 25 participants completed the second MRI scan. Two more participants were excluded from follow-up MRI analyses due to excessive motion on three or more runs. Therefore, pre-post behavioral and MRI analyses included all data from the 23 adults who provided valid data (Fig. 1). Of these 23 adults, 10 were randomized to the active rTMS condition, and 13 received sham stimulation.

2.2. Procedures

After providing voluntary, written informed consent, participants completed diagnostic assessments, a questionnaire packet, and an interview intended to help personalize the emotion regulation intervention (Neacsiu et al., 2022). Participants also identified ten negative and four neutral lifetime memories and rated the arousal and valence elicited by remembering each event (Kross et al., 2009). Each memory was rated along several phenomenological characteristics using an abbreviated version of the Autobiographical Memories Questionnaire (AMQ) (Talarico et al., 2004; Greenberg et al., 2005). Participants then generated a unique verbal descriptor for each memory to be used as a retrieval cue during MRI, as in prior work (Talarico et al., 2004). Autobiographical memories were chosen as a means of emotional induction to more closely mirror the clinical processes targeted by therapeutic interventions.

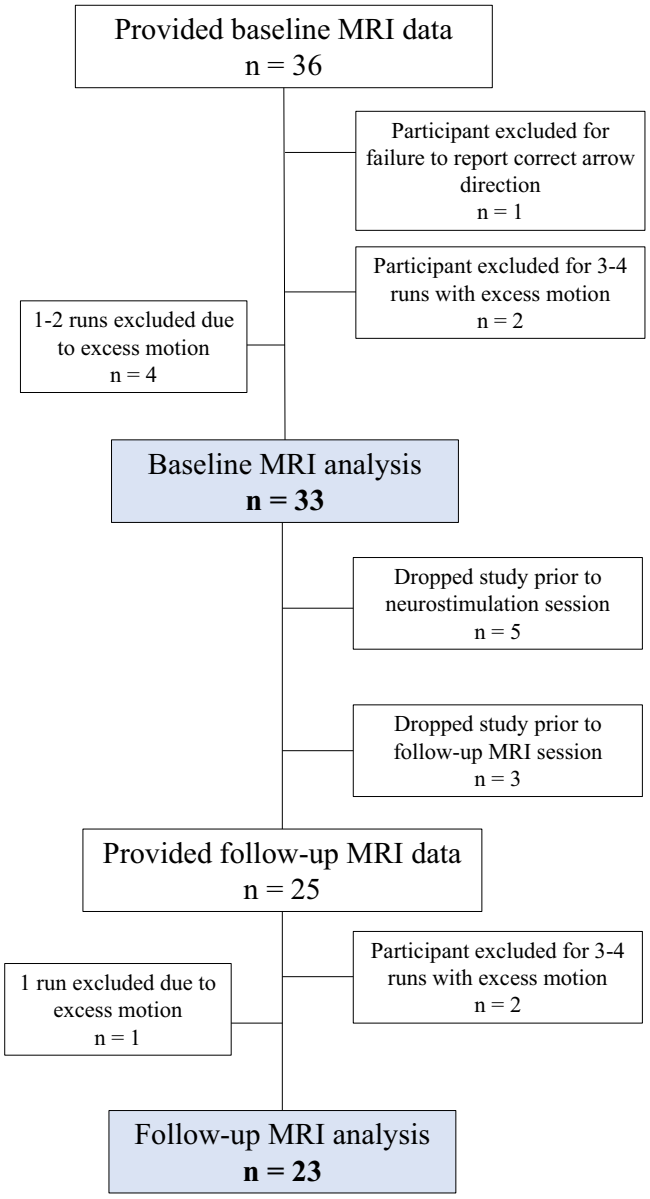

Fig. 1. Diagram of MRI participant flow at the baseline and follow-up session. Excluded participants are indicated on the right, and participants with < 4 runs included in the analysis are indicated on the left.

Over approximately one month, participants were asked to complete a baseline 120-minute MRI session, a TMS intervention session, and a second identical MRI session. During the 3.5-hour intervention session, participants were instructed in CR and practiced this skill on personalized stressors during real or sham rTMS applied at 10 Hz over a personalized left dorsolateral prefrontal cortex (dlPFC) target. Participants could choose either "reframing" or "distancing" to downregulate distress associated with each stressor to increase the ecological validity of the study design, allowing them to use whichever strategy was more accessible to implement for each stressor. Baseline fMRI scan results determined the TMS targets. Participants then completed weekly phone calls, a follow-up MRI, and a one-month follow-up assessment. See (Neacsiu et al., 2022) for details of the TMS and one-month follow-up

Table 1
Demographics and clinical descriptives by group.

	Intake (n = 33)
Mean age (SD)	34.15 (13.74)
Female gender (%)	81.8
Latinx Background (%)	9.1
Racial Background (%)	
Asian/Asian American	15.1
Black/African American	12.1
Native American, American Indian, or Alaskan Native	3.0
White/Caucasian	63.6
Multiracial	6.1
Sexual Orientation (%)	
Heterosexual	72.7
Homosexual	9.1
Bisexual/Questioning	15.1
Total # of Diagnoses, Lifetime (SD)	4.76 (2.18)
Total # of Diagnoses, Current (SD)	3.24 (1.68)
Current Disorders (%)	
Anxiety Disorders	87.9 (n = 29)
Depressive Disorders	30.3 (n = 19)
Lifetime Disorders (%)	
Anxiety Disorders	87.9 (n = 29)
Depressive Disorders	78.8 (n = 26)
Avoidant PD (%)	15.2 (n = 5)
Borderline PD (%)	15.2 (n = 5)
Histrionic PD (%)	6.1 (n = 2)
Obsessive-Compulsive PD (%)	6.1 (n = 2)
Any PD (%)	27.3 (n = 9)

Note. PD = Personality Disorder, SD = Standard Deviation.

sessions, as well as TMS results.

2.2.1. Imaging procedures

At the beginning of each imaging session, participants practiced identifying memories by their cue words until all cues successfully triggered autobiographical memories (Kross et al., 2009; Powers et al., 2019). In addition, they were taught two types of cognitive restructuring: reframing and distancing. Participants were taught that "reframing" involves looking at a situation from a different perspective or thinking of what might come out of the situation to feel less upset. For "distancing," we instructed participants to either look at the situation objectively (like a news reporter), think that the situation happened in a different space, or think that it's a time-limited event or that it's just a memory. Last, we asked participants to let their thoughts and emotions flow naturally without expending efforts to change their experience when being prompted to "feel." Participants practiced these strategies with two standardized scenarios by saying out loud what they would think for the experimenter to check comprehension. Strategies were covered sufficiently for the participant to be able to engage in the targeted behavior during the scan, but not in-depth, such that the participant learned new ways to downregulate emotions. In-depth training in distancing and reframing was performed at the TMS session.

Next, participants moved into the scanner. The scan started with a T1-weighted anatomical image (3D-T1-weighted echo-planar sequence, acquisition matrix = 256 × 256, time repetition [TR] = 2300 ms, echo time [TE] = 3.2 ms, field of view [FOV] = 256 mm^2, in-plane voxel size = 1.0 × 1.0 mm, slice thickness = 1.0 mm, spacing between slices = 0 mm, 162 slices). Four runs of EPI functional images were also acquired with an oblique axial orientation (acquisition matrix = 128 × 128, TR = 2000 ms, TE = 30 ms, FOV = 256 × 256 mm^2, in-plane voxel size = 2.0 × 2.0 mm, slice thickness = 2.0 mm, spacing between slices = 0 mm). Runs 1 and 3 had 240 vol; runs 2 and 4 had 216 vol.

During the functional acquisitions, participants performed 42 trials in total of the emotion regulation task. Each trial of the task (Fig. 2) consisted of sequential presentations of a jittered cross (passive baseline; 6–10 s), a low-level active baseline task (judging whether arrows are pointed to the left or right; 9 s), an autobiographical memory cue word (5 s), and a strategy word ("Feel," "Distance," or "Reframe"; 10 s). After every strategy implementation, participants used the Subjective Units of Distress (SUDS) scale (10 s) to rate distress from 0 (no distress) to 9

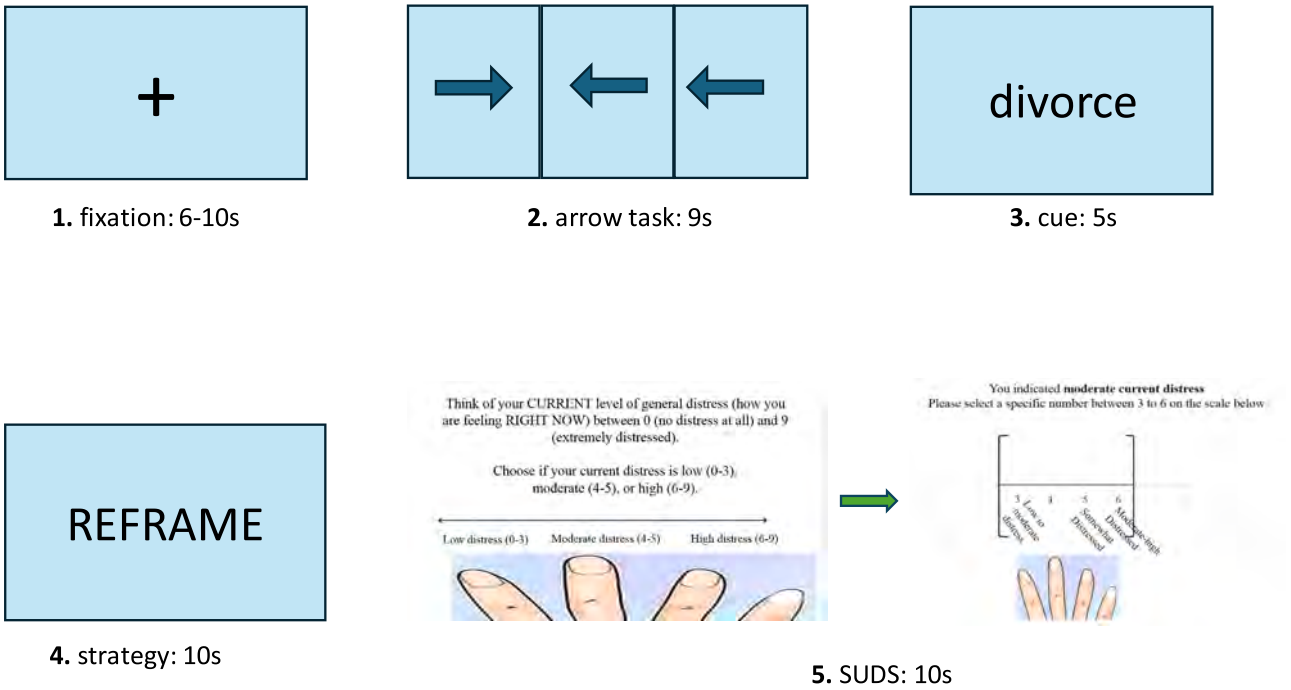

Fig. 2. Example of a task trial. Participants first fixated on a cross (6–10 s, jittered); indicated the direction (left or right) of three arrows in an active baseline task (9 s); were cued to recall a negative or neutral autobiographical memory (5 s); implemented a strategy (reframe, distance, or feel) to either reduce or experience the emotional distress associated with the cue (10 s); and indicated their level of distress (10 s) using two screens intended to capture subjective units of distress (SUDS) ratings between 0 (not distressed at all) and 9 (extremely distressed). Given a 4-button box available in the scanner, SUDS were rated by picking a bucket of distress first (low, moderate, high) and then indicating the specific distress experienced from within that bucket. Participants were trained in this approach to rating distress before the scan.

(highest possible distress) (Wolpe, 1969). When memory cue words were presented (in random order), participants brought the cued memory to mind. Each of the ten negative memories was regulated using each of the three strategies, and the fMRI task was blocked by strategy in a counterbalanced order across participants. The four neutral memories were only combined with the "Feel" strategy and were repeated thrice to be included in each run. Each run had four blocks (feel_negative, feel_neutral, distance_negative, reframe_negative) that were pseudo-randomized, and each block had 2–3 trials. Memories did not repeat within one run. The task involved approximately 35 min in the scanner and has been successfully employed in the past by different research groups (Doré et al., 2018; Smoski et al., 2024).

2.3. Whole-Brain neuroimaging data analysis

Structural and functional data were first examined with MRIQC (Esteban et al., 2017) and preprocessed with fMRIprep1.1.1 (Esteban et al., 2019). Preprocessing steps are described in the Supplement. At the first level, functional data were analyzed as individual runs using a general linear model (GLM) as implemented in FSL's FEAT (Woolrich et al., 2001; Woolrich et al., 2004). Model regressors were created for each trial event described above (see details in Supplement). A weight of 1 was attributed to each task regressor in the GLM. The trial "on" times were convolved with a double-gamma hemodynamic response function to create the final GLM regressors. The "Restructure vs. Feel Negative" contrast was defined as the combination of distancing and reframing instructions minus the "Feel Negative" instructions. Both strategies were combined into one contrast because the study aimed to investigate neural changes associated with the group of techniques that comprise cognitive restructuring (Buhle et al., 2014), and participants could practice either strategy to downregulate distress during the TMS intervention (exploratory follow-up analyses for each strategy separately are also reported). This contrast was then used in the second-level analysis, in which the first-level results for each of the four runs were combined using a fixed-effect model per participant.

Participant-level contrast maps were then carried through to group-level (third level) analyses to model patterns in whole-brain activation for each MRI session. Voxel-wise, mixed-effects analysis was implemented using FLAME 1 in FSL's FEAT. A voxel-wise threshold of $z = 2.3$ was used for all whole-brain group models, and clusters were corrected for multiple comparisons using family-wise error (FWE) correction with a threshold of $\alpha < 0.05$ as part of the standard FSL analysis. These results were then integrated with all other study results and corrected using a Benjamini and Hochberg false discovery rate (FDR) correction (Benjamini and Hochberg, 1995) ($q = 0.10$).

A group analysis explored differences in functional activation/connectivity at the second MRI relative to the first MRI. The same preprocessing steps described above were applied to the follow-up images to generate the 'Restructure vs. Feel Negative' contrast for each participant and each run. To model within-participant differences from pre-intervention to post-intervention, we conducted a single-group paired difference *t*-test analysis using a fixed-effects model with FSL's FEAT tool; second-level analyses (the participant-level average of the four GLMs per run) from both baseline and follow-up were included in this model. Each within-participant pre-intervention to post-intervention change analysis was then examined in a single-group paired difference FSL FEAT analysis using a mixed-effects model (FLAME 1) to assess the differences across all participants and between participants who were assigned to the active versus sham rTMS group. We could, therefore, examine group (active vs. sham) differences in brain activity occurring from pre-intervention to post-intervention while controlling for within-participant effects. This modeling approach was selected because, in FSL, repeated-measures models (i.e., a 2-way mixed effect ANOVA) preclude the examination of group effects, as participants are treated as random effects. Finally, to explore whether the intervention condition was associated with improved emotion dysregulation during 'Restructure vs. Feel Negative,' we calculated the pre-post difference in the DERS score ($DERS_{baseline} - DERS_{1week}$). We included the mean-centered change in emotion dysregulation as a covariate in the group-level between-session analysis.

For all group-level mixed effects models, an initial voxel-wise threshold of $z = 2.3$ was used, and clusters were corrected for multiple comparisons using FWE correction at a threshold of $\alpha < 0.05$. The significant clusters were included with the rest of the results and subjected to FDR corrections.

2.4. Measures

2.4.1. Self-reports

The abbreviated AMQ examined subjective arousal, valence, vividness, memory rehearsal, and age for the negative and neutral memories included in the imaging experiment. The cognitive reappraisal subscale of the ERQ (Gross and John, 2003), the 8-item version of the Patient-Reported Outcomes Measurement Information System v1.0-Self-Efficacy for Managing Emotions (PROMIS-SEME)(53, 54) and the DERS (Gratz and Roemer, 2004) captured self-reported emotional regulation and dysregulation. Specifically, the ERQ Reappraisal scale (i.e., reappraisal proficiency) and the PROMIS-SEME total score (i.e., emotion regulation self-efficacy) were used to measure emotional regulation. The ERQ Reappraisal scale (Gross and John, 2003) includes items rated on a 7-point Likert scale to identify how likely one is to use cognitive reappraisal to alter positive and negative emotions, with responses ranging from one (*strongly disagree*) to 7 (*strongly agree*). The PROMIS-SEME assesses a participant's level of confidence in managing anxiety, stress, discouragement, disappointment, distress, and negative feelings (Gruber-Baldini et al., 2017; Lee et al., 2019) on a 1–5 Likert scale (1 = *I* am not at all confident; 5 = *I* am very confident). In contrast, the DERS captures emotional dysregulation and includes several subscales that tap into various difficulties with emotional management (e.g., lack of effective strategies, clarity, not accepting emotional experiences, etc.; see Supplement for more details). Participants rate 36 items on a Likert scale ranging from 1 (*almost never*) to 5 (*almost always*), and the total sum score indicates high dysregulation. These measures were collected at both baseline and follow-up.

2.4.2. Neuroimaging outcome measures

2.4.2.1. Anatomical region of interest activation. All anatomical regions of interest (ROIs) were identified using the Brainnetome Atlas (Fan et al., 2016) modeling the PFC ROIs (dlPFC, dmPFC, vlPFC, vmPFC, and OFC) after a review article (Carlén, 2017) that parcellated the PFC by functional divisions, including all subdivisions in the insula and amygdala ROIS. ROIs were corrected using the AFNI 3dmask_tool to fill in any gaps between the gray matter patterns and multiplied with a participant-specific intensity-based mask applied to each participant's functional data (Peer et al., 2016) aimed to remove signal attenuation effects.

If whole brain analyses did not yield significant findings in pre-specified brain regions of interest (ROIs) as well as for correlational analyses, we used FSL's "featquery" to extract parameter estimates from each participant's second-level statistical maps within the relevant a priori intensity-masked anatomical ROI. Specifically, the parameter estimate was the average activation within a 6-mm sphere centered at the voxel with the maximum activation difference within the contrast of interest (Tong et al., 2016).

2.4.2.2. Functional region of interest (fROI) metric. General psychophysiological interaction (gPPI) (McLaren et al., 2012) analysis was used to investigate brain regions showing task-dependent activation synchronicity with seed regions containing significant [Restructure - Feel Negative] contrast values. Functional ROIs were created within the a

priori anatomical ROIs. Using "fslmaths," we extracted significant BOLD activation ($z > 2.3$) during [Restructure – Feel Negative] from each a priori intensity-masked ROI for each participant and binarized these data to create a participant-level functional mask. We then added all participants' fROIs to create a group-level fROI that was anatomically constrained (Nieto-Castañón and Fedorenko, 2012). The overlap threshold (minimum proportion of participants showing activation at each voxel) was 10%, meaning that voxels with fewer than 10% of participants showing activation were excluded from each group-level fROI. Using a generalized PPI approach in which all main effects of the task were modeled in addition to interaction effects allowed us to circumvent circularity within the analysis; only functional connectivity effects orthogonal to the task's main effect were detected (O'Reilly et al., 2012). Details of the PPI analyses can be found in the Supplement. We examined connectivity using the left and right dlPFC, left and right amygdala, and left and right insula as seeds (six seeds/analyses in total). For all third-level models, a voxel-wise threshold of $z = 2.3$ was used, and clusters were corrected within the FSL analysis for multiple comparisons using FWE correction at a threshold of $\alpha < 0.05$. These results were included with the rest of our findings and subjected to an FDR correction.

2.5. Statistical analyses

Analyses were conducted using SPSS version 25.0. To account for multiple comparisons, we adjusted the significance for analyses from both Aims using an FDR correction (Benjamini and Hochberg, 1995) ($q = 0.10$). See Supplement for more details.

3. Results

3.1. Memory phenomenology

At baseline, instructions to experience emotions prompted by autobiographical memories yielded SUDS ratings that were normally distributed (Shapiro Wilk $W = 0.92, p < .001$). There were no significant baseline differences in distress ratings of the autobiographical memories as a function of group assignment (sham vs. active TMS), $F\ (1, 25.97) = 0.003$, $p = .95$. Distress elicited by negative autobiographical memories (in the absence of regulation) decreased significantly from baseline to follow up, $F\ (1, 184.29) = 23.70$, $p_{FDR} = 0.004$, with no difference between conditions, $F\ (1,87.50) = 0.02$ $p = .90$.

A linear regression analysis showed that the AMQ scores significantly predicted negative arousal $F\ (5, 417) = 182.28$, $p < .000000001$), explaining 68.6% of the variance in self-reported SUDS scores following negative emotion induction during the baseline MRI scan. Examining individual AMQ predictors, we found that valence ($\beta_{valence} = -0.42$, $p_{FDR} = 0.0042$), arousal ($\beta_{arousal} = 0.48$, $p_{FDR} = 0.0006$), and vividness ($\beta_{vividness} = 0.14$, $p_{FDR} = 0.0095$) significantly predicted the distress induced by remembering negative and neutral memories during the baseline MRI scan. Therefore, these variables were added as co-variates in the subsequent analysis. Memory age and rehearsal were not significant predictors ($ps > 0.69$) and were not included in subsequent analyses.

3.2. Brain circuitry associated with emotion regulation and dysregulation

3.2.1. Functional activity at baseline

The whole-brain analysis of the 'Restructure vs. Feel Negative'

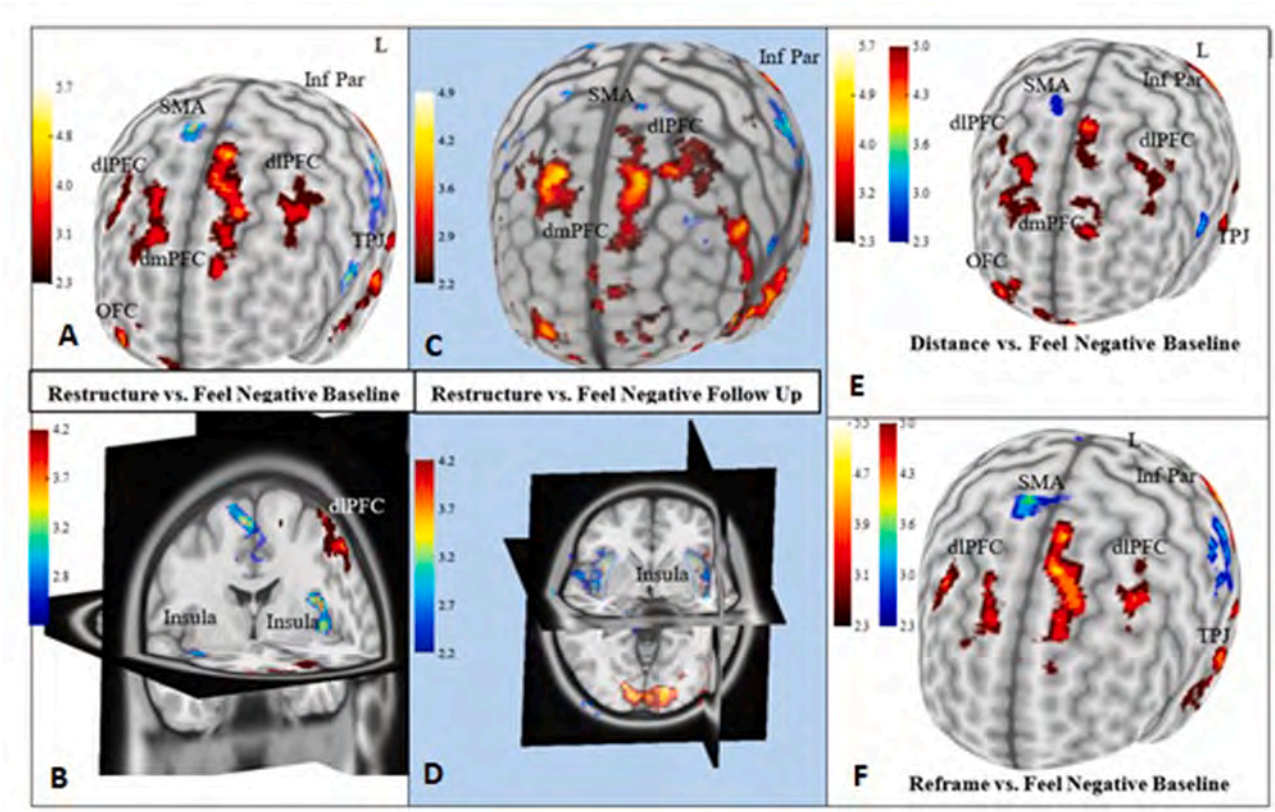

Fig. 3. Whole-brain fMRI activation results during emotion regulation. Hot colors indicate significantly increased activity, whereas cool colors indicate significantly decreased activity. SMA = supplementary motor area; dlPFC = dorsolateral prefrontal cortex; dmPFC = dorsomedial prefrontal cortex; OFC = orbitofrontal cortex; Inf Par = inferior parietal cortex; TPJ = temporoparietal junction. (A and B) Brain regions with activation changes in the Restructure > Feel Negative contrast during baseline scanning. (C and D) Similar activation patterns are found in A and B but at the follow-up scan. (E) The strategy-specific activation pattern in the Reframe > Feel Negative contrast at baseline. (F) Same as in E but for the Distance > Feel Negative contrast.

contrast revealed significant activation clusters in the bilateral dlPFC and dmPFC, the left inferior parietal cortex, and the temporoparietal junction (TPJ, Fig. 3; Table 2). Significant de-activation from the same contrast was seen in the bilateral supplementary motor area (SMA), bilateral insula, the right midcingulate cortex, right vlPFC, and the left posterior cingulate cortex (Fig. 3; Table 2). Because no changes in the amygdala were detected using whole-brain analyses, we conducted a one-sample *t*-test ROI analysis to examine changes in this region during regulation. These exploratory results indicated significant amygdala activation during regulation (restructure> feel negative; $M_{amygdala\_average\_peak\_activation} = 0.15$, SD = 0.11, t (30) = 7.09, $p_{FDR} = 0.0016$).

Table 3 displays results from the brain-behavioral correlation analyses. Higher activation in the right vmPFC during regulation compared to emotional induction was correlated with less proficiency with reappraisal and with higher emotional dysregulation (specifically with limited access to emotion regulation strategies). Furthermore, higher activity in the left amygdala during regulation positively correlated with higher emotional dysregulation. Of the facets of emotional dysregulation, left amygdala activation was significantly associated with limited access to emotion regulation strategies and difficulties engaging in goal-directed behaviors.

3.2.2. Connectivity at baseline

Results from the seed-based whole-brain PPI analyses revealed significant connectivity findings linking the right insula (seed) to the left midcingulate cortex ($Z_{max} = 3.97$; $p_{FDR} = 0.0044$; $x = -10.5$, $y = -36.5$, $z = 47.5$; Fig. 4) during emotion regulation. A one-sample *t*-test indicated significant dlPFC-amygdala connectivity during regulation ($M_{dlPFC\text{-}amygdala\_connectivity} = 0.23$, SD = 0.19, t (32) = 6.69, $p_{FDR} = 0.0020$). ROI-to-ROI PPI data analyses found a significant positive correlation between difficulties with emotion regulation and the left insula-right dlPFC connectivity, right insula–right vlPFC connectivity, and right amygdala-right OFC connectivity. From the DERS subscales, limited access to emotion regulation strategies significantly correlated with the insula connectivity patterns and the right amygdala-right OFC connectivity. Difficulties in goal-directed behaviors correlated with the left insula – right dlPFC connectivity. Difficulties with impulse control when distressed correlated with the right amygdala-right OFC connectivity (Table 3).

Proficiency with reappraisal was negatively correlated with the bilateral dlPFC-left OFC, right dlPFC-left dlPFC, right insula-left OFC, left insula-right vmPFC, and right dlPFC-left vlPFC connectivity. Finally, self-efficacy with emotion regulation (as indicated by the PROMIS-SEME total score) was negatively correlated with the right insula-left OFC connectivity and with the right dlPFC-left dmPFC connectivity (Table 3). Strategy-specific results are detailed in the Supplement.

3.3. The effect of the pilot intervention on neural markers of emotion regulation

3.3.1. Change in functional activity at follow-up

Whole-brain and ROI analyses found no differences between intervention conditions when examining changes from intake to follow-up in activation during cognitive restructuring versus feeling negative emotions associated with autobiographical memories (*ps* > 0.05; Fig. 3 shows whole-brain data from both phases). FDR-corrected ROI analyses

Table 2
Areas of significant activation at baseline following whole brain analyses[i].

CONTRAST	CLUSTER INDEX	vOXELS	P_{FDR}	Z-MAX	Z-MAX X (MM)	Z-MAX Y (MM)	Z-MAX Z (MM)
RESTRUCTURE > FEEL NEGATIVE	Bilateral fusiform gyri	13,821	0.0002	5.66	21.5	−84.5	−14.5
	Left angular gyrus	2151	0.0009	5.12	−48.5	−60.5	35.5
	Left SMA	1150	0.0025	4.56	−8.5	5.5	63.5
	Right dmPFC	1064	0.0026	4.33	19.5	39.5	53.5
	Right angular gyrus	639	0.0047	3.49	55.5	−62.5	39.5
	Left dlPFC	585	0.0050	4.25	−42.5	19.5	47.5
FEEL NEGATIVE > RESTRUCTURE	Right mid-cingulate cortex	1383	0.0014	3.93	3.5	3.5	45.5
	Left insula	510	0.0055	4.1	−38.5	1.5	11.5
	Left supramarginal gyrus	480	0.0061	3.55	−60.5	−42.5	37.5
	Left posterior cingulate cortex	415	0.0084	4.21	−8.5	−34.5	43.5
	Right insula	313	0.0128	3.29	43.5	−12.5	−6.5
DISTANCE > FEEL NEGATIVE	Bilateral occipital cortex	13,348	0.0003	5.71	25.5	−86.5	−16.5
	Left angular gyrus	1950	0.0012	4.72	−46.5	−60.5	35.5
	Right dmPFC	1085	0.0028	4.28	23.5	31.5	57.5
	Right vmPFC	827	0.0039	4.55	27.5	61.5	1.5
	Right angular gyrus	621	0.0048	4.3	31.5	−74.5	49.5
	Corpus callosum, left side	434	0.0076	4.07	−12.5	25.5	11.5
	Left dlPFC	424	0.0079	3.49	−40.5	3.5	41.5
	Left SMA	309	0.0134	4.18	−6.5	3.5	65.5
FEEL NEGATIVE > DISTANCE	Right mid-cingulate cortex	903	0.0034	5.02	1.5	5.5	45.5
	Left insula	436	0.0075	4.49	−42.5	−0.5	9.5
REFRAME > FEEL NEGATIVE	Bilateral occipital cortex	8656	0.0005	5.54	−46.5	−76.5	−12.5
	Left angular gyrus	1166	0.0023	4.92	−46.5	−52.5	25.5
	Left dmPFC	1083	0.0030	5.19	−8.5	17.5	57.5
	Left posterior cingulate cortex	669	0.0045	4.18	−0.5	−50.5	27.5
	Right dmPFC	469	0.0064	4.33	17.5	39.5	53.5
	Left temporal pole	458	0.0072	4.78	−56.5	11.5	−22.5
	Right angular gyrus	357	0.0109	3.67	51.5	−52.5	35.5
	Left dlPFC	330	0.0115	4.37	−42.5	19.5	47.5
	Left hippocampus	301	0.0143	4.07	−26.5	−30.5	−4.5
FEEL NEGATIVE > REFRAME	Right SMA	1272	0.0017	4.21	11.5	−6.5	73.5
	Right temporal operculum	1199	0.0019	4.05	55.5	−16.5	11.5
	Left posterior cingulate cortex	1033	0.0031	4.97	−12.5	−36.5	45.5
	Right posterior middle temporal gyrus	462	0.0069	4.72	49.5	−68.5	11.5
	Left supramarginal gyrus	428	0.0078	3.52	−66.5	−42.5	37.5

Note. [i]For all whole-brain group models, a cluster-forming voxel-wise threshold of $z = 2.3$ was used, and clusters were corrected for multiple comparisons at a threshold of $p < .05$; The resulting significant clusters were combined with the rest of the results and corrected with FDR. Only FDR significant results are presented here. SMA = supplementary motor area, dmPFC = dorsomedial prefrontal cortex, dlPFC = dorsolateral prefrontal cortex, vmPFC = ventromedial prefrontal cortex, OFC = orbitofrontal cortex.

Table 3
Associations between emotion regulation characteristics and neural activity or connectivity during Restructure vs. Feel Negative contrast.

Analysis	*Seed*	*Connected Region*	*Measure*	*R*	p_{FDR}
INTAKE					
Activation	Left amygdala	–	Difficulties with emotion regulation	0.485	.0111
		–	- Limited access to emotion regulation strategies	0.583	.0067
		–	- Difficulty engaging in goal-directed behavior	0.449	.0131
Activation	Right vmPFC	–	Reappraisal proficiency	−0.536	.0081
Activation	Right vmPFC	–	Difficulties with emotion regulation	0.589	.0058
			- Limited access to emotion regulation strategies	0.495	.0103
FC	Left insula	Right dlPFC	Difficulties with emotion regulation	0.574	.0062
			- Limited access to emotion regulation strategies	0.584	.0059
			- Difficulty engaging in goal-directed behavior	0.517	.0090
FC	Left Insula	Right vmPFC	Reappraisal proficiency	−0.430	.0145
FC	Right insula	Right vlPFC	Difficulties with emotion regulation	0.498	.0101
			- Limited access to emotion regulation strategies	0.569	.0065
FC	Right insula	Left OFC	Reappraisal proficiency	−0.473	.0112
FC	Right insula	Left OFC	Emotion regulation self-efficacy	−0.459	.0126
FC	Right amygdala	Right OFC	Difficulties with emotion regulation	0.435	.0132
			- Limited access to emotion regulation strategies	0.424	.0142
			- Difficulties with impulse control	0.450	.0123
FC	Left dlPFC	Left OFC	Reappraisal proficiency	−0.498	.0117
FC	Right dlPFC	Left OFC	Reappraisal proficiency	−0.446	.0098
FC	Right dlPFC	Left dlPFC	Reappraisal proficiency	−0.508	.0100
FC	Right dlPFC	Left vlPFC	Reappraisal proficiency	−0.436	.0139
FC	Right dlPFC	Left dmPFC	Emotion regulation self-efficacy	−0.450	.0140
CHANGE AT FOLLOW-UP					
Activation	Right OFC	–	Improved reappraisal proficiency	−0.640	.0107
FC	Left dlPFC	Right dmPFC	Improved emotion regulation self-efficacy	−0.710	.0070
FC	Left insula	Right dmPFC	Improved emotion regulation self-efficacy	0.586	.0121
FC	Left insula	Left vlPFC	Improved emotion regulation self-efficacy	0.564	.0136
FC	Left insula	Left vlPFC	Improved reappraisal proficiency	0.569	.0129
FC	Right insula	Right vlPFC	Improved reappraisal proficiency	0.588	.0120

Note. FC = functional connectivity; vmPFC = ventromedial prefrontal cortex; dlPFC = dorsolateral prefrontal cortex; OFC = orbitofrontal cortex; vlPFC = ventrolateral prefrontal cortex; dmPFC = dorsomedial prefrontal cortex; r = Pearson's r correlation coefficient (partial correlation for follow up changes); p = uncorrected significance for correlation analysis; p_{FDR} = FDR corrected significance value. Reappraisal proficiency refers to the emotion regulation questionnaire cognitive restructuring scale average score; emotion regulation self-efficacy refers to the total score on the PROMIS-SEME scale. These measures were collected at both baseline and follow-up, and improvements indicate change scores in the desired direction in these behavioral measures. Changes in activation and connectivity indicate differences from baseline in the regions of interest and their connections. All changes in this table are collapsed across treatment groups.

showed that in all participants, improved proficiency with reappraisal was correlated with lower activity in the right OFC at follow-up (Table 3).

3.3.2. Change in connectivity at follow-up

Seed-based whole-brain voxel-wise PPI analyses revealed a significantly higher increase, from baseline to follow-up, in functional connectivity between right occipital cortex and right insula (seed; Z_{max} = 3.28; p_{FDR} = 0.0093; x = 25.5, y = −92.5, z = −6.5) as well as between right occipital cortex and left dlPFC (seed; Z_{max} = 3.73; p_{FDR} = 0.0118; x = 37.5, y = −82.5, z = −0.5) in the active versus the sham condition, when participants were engaged in cognitive restructuring. ROI-to-ROI analyses also found a significantly higher increase, from baseline to follow-up, in connectivity during regulation in the active versus the sham condition between right dlPFC (seed) and right OFC (t(21) = 3.22, p_{FDR} = .0106) and between left dlPFC and left insula (t(21) = 2.75, p_{FDR} = .0137).

Across all participants, FDR-corrected whole brain analyses found a significant increase in connectivity during 'Restructure vs. Feel Negative' between right amygdala and left anterior insula at follow-up when compared to baseline (Z_{max} = 3.58; p_{FDR} = 0.0089; x = −22.5, y = 25.5, z = −10.5). ROI-to-ROI correlational analyses showed that improved self-efficacy in managing emotions was correlated with a decreased connectivity between the left dlPFC and right dmPFC and increased connectivity between the left insula and left vlPFC and right dmPFC. We also found that improvements in reappraisal proficiency were correlated with increased connectivity between the right insula and right vlPFC and between the left insula and left vlPFC (Table 3).

3.3.3. Intervention-related improvement in emotion dysregulation

In the whole-brain analysis, we found a significant three-way interaction between group, session, and change in DERS score at follow-up; when compared to baseline, more significant improvement in emotion dysregulation was associated with decreased left vlPFC (454 voxels; Z_{max} = 4.47; p_{FDR} = 0.0053; x = −48.5, y = −26.5, z = −0.5) and left superior temporal gyrus (294 voxels; Z_{max} = 3.84; p_{FDR} = 0.0114; x = −50.5, y = 23.5, z = −2.5) activation in the active rTMS group compared to the sham group. The interaction between group x session x emotion dysregulation improvement using functional connectivity was also significant; at follow-up compared to intake, more remarkable improvement in emotion dysregulation in the active group compared to

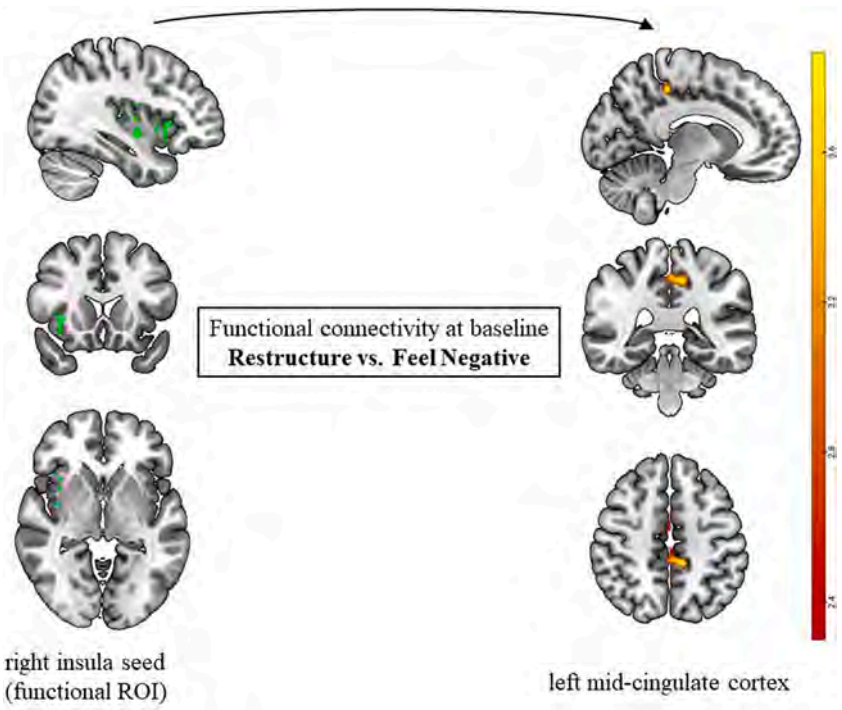

Fig. 4. Functional connectivity between the right insula and the left mid-cingulate cortex (voxel threshold: $z = 2.3$, cluster-correction threshold: $p < .05$) in the Restructure> Feel Negative contrast at the baseline MRI scan. The right insula functional ROI seed indicated in green includes voxels activated in the Restructure > Feel Negative contrast in at least 10% of participants.

sham was associated with decreased connectivity between the right dlPFC (seed) and left inferior parietal lobule (319 voxels; $Z_{max} = 3.19$; $p_{FDR} = 0.0097$; $x = -60.5$, $y = -46.5$, $z = 41.5$), and increased connectivity between the right OFC (seed) and left cerebellum (341 voxels; $Z_{max} = 4.09$, $p_{FDR} = 0.0087$; $x = -18.5$, $y = -68.5$, $z = -30.5$).

3.4. The effect of the pilot intervention on behavioral markers of emotion regulation

3.4.1. Changes in behavioral markers of emotion regulation

Change in distress following regulation prompts when compared to experience emotions prompts at follow-up was normally distributed (Shapiro Wilk $W = 0.96$, $p < .001$). At follow-up, a small proportion of the entire pool of 250 negative memories (19 memories in the sham TMS group, 27 memories in the active TMS group) no longer induced significant distress (i.e., SUDS ratings following Feel Negative block missing or ≤ 1). Emotion induction is necessary to capture emotion regulation. Therefore, we present behavioral results that exclude trials where memories that no longer induced arousal were presented (the analysis that does not exclude these trials is presented in the Supplement).

When including only memories that successfully elicited emotional arousal ($SUDS_{following\_FEEL} > 1$), an MMANOVA using an autoregressive covariance structure found a significantly higher reduction in SUDS when engaging in downregulation versus when simply experiencing emotions associated with negative autobiographical memories in the active versus the sham condition, $F[1, 140.66] = 11.42$, $p < .00094$, $p_{FDR} = 0.0073$. Participants who received active neurostimulation ($EMM_{delta\_suds\_active} = 1.96$, $S.E. = 0.18$) reduced their distress more following instructions to downregulate versus feel than participants who received sham neurostimulation ($EMM_{delta\_suds\_sham} = 1.32$, $S.E. = 0.19$), with a small effect size ($d = 0.36$). There was no difference in the effectiveness of emotion regulation between employed tactics, F (1, 208.67) = 0.25, $p = .62$. Baseline SUDS (Parameter $Estimate_{delta\_suds\_intake} = 0.27$, $S.E. = 0.05$, $p_{FDR} = 0.0033$), average ratings following neutral memories (Parameter $Estimate_{average\_suds\_neutral} = -0.54$, $S.E. = 0.10$, $p_{FDR} = 0.0037$), and baseline use of cognitive restructuring (Parameter $Estimate_{ERQ\_Reappraisal\_intake} = 0.39$, $S.E. = 0.07$, $p_{FDR} = 0.0036$) were also significant predictors of regulation success at follow up. Ratings from the autobiographical memory questionnaire for arousal, valence, and vividness were not significant predictors of follow-up regulation success ($ps > 0.05$).

4. Discussion

The first aim was to characterize the brain circuitry associated with emotional regulation and dysregulation in a transdiagnostic clinical sample. Group maps of neural activation during CR versus simply experiencing emotions showed the expected involvement of several hypothesized prefrontal regions (dlPFC, dmPFC, vmPFC), inferior parietal cortex, and TPJ. We also found decreased activation in the bilateral insula with whole brain analyses and increased amygdala activity in ROI analyses. In contrast to consistently reported increased activation of the vlPFC and SMA during emotion regulation in healthy controls (Kohn et al., 2014; Morawetz et al., 2017; Li et al., 2021), we found decreased activation in the right vlPFC and bilateral SMA during regulation in our clinical sample [consistent with other clinical studies (Wang et al., 2008)]. Both the vlPFC and the SMA are thought to act as relay stations between subcortical and prefrontal regions (Wager et al., 2008); they receive emotional arousal information from subcortical regions, participate in strategy selection, and facilitate top-down implementation of regulation by the dlPFC (Silvers et al., 2013; Morawetz et al., 2016). Therefore, a marker of dysregulation may be insufficient synchronized input between subcortical and cortical regions, a hypothesis supported by studies showing increased activation in these regions after treatment (MacNamara et al., 2016; He et al., 2023).

Following the one-time pilot intervention, we found that cognitive restructuring in the active rTMS group (compared to the sham group) significantly increased functional connectivity between the right insula and the right occipital cortex, as well as between the left dlPFC and the

right occipital cortex. These group-specific effects should be considered preliminary, given the small sample sizes. Across all participants (irrespective of group assignment), we saw increased connectivity between the right amygdala and insula and the left midcingulate cortex, with no changes in activation patterns. These connectivity effects are likely due to the CR training, which was common across the two groups. Altogether, the connectivity results highlight the importance of interactions between the salience and default-mode brain networks as a potential marker of intervention success and the critical role of the insula in emotion regulation.

4.1. Neural metrics associated with emotional dysregulation

Our initial hypothesis was that hypoactivation in the dlPFC and problematic connectivity patterns between the PFC and limbic regions were markers of emotional dysregulation. Our findings only partially aligned with our hypotheses. Activation in the left amygdala during regulation was correlated with limited access to emotion regulation strategies and difficulties engaging in goal-directed behaviors. A recent meta-analysis of functional connectivity studies during emotion regulation highlighted that the right dlPFC, left vlPFC, and right dmPFC consistently correlate with the amygdala when non-clinical participants downregulate using reappraisal (Berboth and Morawetz, 2021). Thus, a possible mechanism of emotional dysregulation is insufficient synchrony between the amygdala and these PFC regions during regulation. This stems from limited access to emotion regulation strategies and an inability to regulate when upset.

Interestingly, right amygdala-right OFC connectivity was associated with poor impulse control in emotional situations. Others have found heightened connectivity between these regions in bipolar disorder adults when exposed to negative stimuli compared to non-clinical controls (Morawetz et al., 2017). In our study, a decrease in OFC activation was correlated with improved reappraisal proficiency at follow-up. These findings suggest that over-involvement of the right OFC and recruitment of this region to downregulate the right amygdala may be another possible marker of emotional dysregulation that can be targeted with treatment.

The strength of the functional connectivity during restructuring between the insula and the right dlPFC/vlPFC was correlated with limited access to emotion regulation strategies. Furthermore, the connectivity between the right insula and the left OFC was also correlated with poor reappraisal skills and low proficiency with emotion regulation. Unlike the amygdala, there are relatively fewer examinations of the role of insula connectivity in emotion regulation. Prior findings suggest that the insula integrates sensory information, including interoceptive awareness, to yield a coherent representation of the experienced emotion (Cauda et al., 2012; Zaki et al., 2012). Others have shown that connectivity between the insula and the vlPFC is correlated with improved reappraisal (Li et al., 2021), while connectivity between the insula and the dlPFC is connected to negative rumination (Li et al., 2022). These findings highlight that problematic insula connectivity with PFC is another marker of emotional dysregulation, the specifics of which are nuanced. It is possible that ineffective coupling between the insula and the left vlPFC impairs the emotion regulation process. Furthermore, the specific ways viscero-sensory input is processed within working memory may be maladaptive in emotionally dysregulated adults.

We did not find activity in the dlPFC correlated with dysregulation behavioral indices. Nevertheless, we found that during restructuring, synchronous activity between the right dlPFC and several other left PFC regions (OFC, dlPFC, vlPFC, and dmPFC) correlated with several indices of emotional dysregulation. We interpret these findings to suggest that, for clinical adults with high emotional dysregulation, there may be a lack of efficiency in the PFC when required to engage in emotion regulation. Other studies have found that reappraisal engages the dmPFC and vlPFC to modulate limbic arousal in normative emotion regulation (Li et al., 2021). Nevertheless, the functional connectivity between prefrontal regions was not examined. Thus, emotional dysregulation may be related less to hypoactivity and instead to aberrant use of resources by neural centers that are not specialized in tasks needed for regulation. In support of this explanation was also our finding that reduced connectivity during regulation between the left dlPFC and right dmPFC at follow-up was associated with improved emotion regulation self-efficacy.

4.2. Neural metrics associated with effective emotion regulation

Although we included participants with various levels of cognitively mediated emotion regulation proficiency, we did not find any neural indices correlating with behavioral indicators of effective emotion regulation at baseline. Nevertheless, we found several markers of emotion regulation when examining changes from baseline following CR training. In particular, connectivity between the insular cortex and the vlPFC correlated with improvements in emotion regulation. A recent causal examination of the role of the vlPFC in emotion regulation found that the left vlPFC may be involved in selecting appropriate reappraisals, while the right vlPFC inhibits inappropriate negative thoughts generated by the emotion (Cheng et al., 2022). As we indicated before, others have found the right vlPFC-right insula connectivity to be predictive of improved reappraisal (Li et al., 2021). Our baseline results lead us to hypothesize that improved emotion regulation is linked with increased efficiency of the right vlPFC in inhibiting insular inputs that promote negative affect. This suggests that how the vlPFC and insula interact could be a key mechanism for improving emotion regulation. These implications could open new avenues for research and potential therapeutic interventions.

In addition, we found that enhanced connectivity between the right dmPFC and the left insula and decreased connectivity between the right dmPFC and the left dlPFC also correlated with improvements in emotion regulation indices. Others have shown that the dmPFC has a critical role in evaluating and interpreting others' mental states and intentions as they relate to one's well-being (Dixon et al., 2017). The dmPFC also appears to be integral to emotional episodic memory processing, acting as an integrator of cognitive and affective domains of functioning throughout memory encoding, stabilization, and retrieval (Kensinger and Ford, 2021). This essential contribution to the affective tone of memories based on narrative context and memory valence is directly relevant to our negative emotional autobiographical memory paradigm in adults with clinical emotion dysregulation.

Aberrant functional activity and connectivity involving the dmPFC during emotion regulation fMRI paradigms have been observed in non-clinical (Berboth and Morawetz, 2021; Frank et al., 2014) and clinical populations (Taylor and Liberzon, 2007; Kjærstad et al., 2022). Of particular interest is a meta-analysis (Berboth and Morawetz, 2021) ($n = 783$) of brain abnormalities in adolescents with transdiagnostic aggressive behavior, which reported congruence in structural and functional abnormalities solely in the right dmPFC and the left insula. These findings suggest that the right dmPFC may be an important treatment target for emotional regulation interventions across the lifespan.

4.3. Effects of the pilot intervention on brain and behavior: preliminary conclusions

The study's second aim was to compare the brain and behavioral effects of a one-time pilot intervention that included teaching and practicing cognitive restructuring paired with real or sham neurostimulation. Given the small sample sizes in each treatment group, these findings should be considered preliminary. When compared with those who received sham, participants who received active neurostimulation improved their ability to downregulate distress during a behavioral emotion regulation task. These results extend our prior findings from this data set, which showed that over the week after neurostimulation,

participants in the active condition used more CR than participants in the sham condition (Neacsiu et al., 2022). Thus, in naturalistic settings and laboratory-based emotion regulation tasks, neurostimulation enhances the utility of a newly acquired behavioral skill in clinical populations.

We explored differences between active and sham conditions during regulation at a neural level using change scores (follow-up – baseline) in both functional activity and connectivity. We found a significantly higher increase in the active vs. sham condition in connectivity between the visual cortex, the left dlPFC, and the right insula. The centrality of visual cortex connectivity during regulation may reflect changes in the imaginal processing of salient negative emotional stimuli (Bradley et al., 2003; Mickley and Kensinger, 2008). Differences between clinical and non-clinical groups in occipital cortex activation have also been reported during the processing of negative emotional stimuli (Hendler et al., 2001; Kearney et al., 2023). Therefore, post-intervention increases in both activation and connectivity of the visual cortex suggest that the interplay between visual imagery and cognitive processing may underlie more efficient emotion regulation in clinical populations.

Participants in the active condition also evidenced higher connectivity at follow-up between the right dlPFC and the right OFC, as well as between the left dlPFC and the left insula. In Aim 1, we showed that the right OFC may be hyperactive in emotional dysregulation, and its connectivity with the right amygdala may be a marker of difficulties with impulse control when upset. The role of connectivity between the amygdala and the OFC in emotional processing is well-established in non-clinical (Fulwiler et al., 2012; Rolls et al., 2023) and clinical (Bachevalier and Loveland, 2006; Versace et al., 2010; Sonkusare et al., 2022) populations.

Frameworks that categorize emotion regulation as implicit (i.e., automatic) or explicit (i.e., effortful) have proposed that explicit regulation methods such as reappraisal rely on the dlPFC to downregulate emotion reactivity regions such as the amygdala and the insula, while implicit regulation depends on the modulation of these regions by medial and orbitofrontal divisions of the PFC (Etkin et al., 2015; Johnstone and Walter, 2014; Braunstein et al., 2017). Critically, synergism and flexibility between these two regulation techniques involve effective interaction between the dlPFC and OFC (Etkin et al., 2015). These preliminary findings suggest that an active treatment mechanism may be improved downregulatory control of the right OFC from the right dlPFC. This, in turn, may reduce the aberrant connection between the right OFC and the right amygdala, reducing impulsivity. Our results indicate that therapeutic intervention may increase efficiency in balancing automatic regulation with a more effortful cognitive reappraisal strategy; this circuitry is worthy of further examination in adults with dysregulation.

Finally, we observed significant differences in post-intervention improvement in emotion dysregulation in the active rTMS group compared to sham; specifically, decreases in left vlPFC and left superior temporal gyrus activity, decreases in connectivity between the right dlPFC and left inferior parietal cortex, and increases in connectivity between the right OFC and left cerebellum. These post-intervention changes in pre-frontal activation and connectivity show the effects of active neuromodulation on the homeostatic rebalance of the control network, perhaps reflecting a reduction in effort needed to reappraise emotions successfully. Studies have shown that the cerebellum is involved in the emotional processing of negative episodic memory and that neuromodulatory inhibition of the cerebellum has been shown to increase negative affect (Baumann and Mattingley, 2012; Schutter and Van Honk, 2005); our results, therefore, support a role for rTMS-modulated augmentation of emotion regulation via medial PFC interactions with major subcortical structures.

4.4. Limitations

As mentioned above, given our small sample size, the effects of the treatment group should be considered cautiously. In addition, we did not include a non-clinical control group, and thus, inferences made regarding clinical vs. non-clinical regulation depended upon comparisons to results in the prior literature. Another limitation of generalizability is the female gender predominance in our sample, which may reflect gender differences in experience and regulation of negative affect, cultural stereotypes of emotional processing, and/or underreporting of emotional difficulties by males rather than true differences in the prevalence of emotion dysregulation as measured by the DERS (Giromini et al., 2017). Studies examining the intersection of gender and emotion regulation find that women and men tend to differ in the type of maladaptive strategies they employ for regulation, with men preferring alcohol use (Nolen-Hoeksema, 2012). In addition, women seek treatment more than men for emotional difficulties (Skodol and Bender, 2003). In our study, alcohol use disorder was excluded because of the possible risk of seizure during rTMS, which may have biased our sample toward women, who are also easier to recruit in emotion regulation studies. Therefore, future studies that explore gender differences and prioritize recruitment of men are warranted to ensure that the neuroimaging results are generalized to non-female segments of the population. Finally, while the study is innovative and has good ecological validity in using autobiographical memories as stimuli, these stress cues are relatively less well controlled and may have introduced variability across participants that affected the results.

5. Conclusion

Targeted interventions for emotional disorders are likely to be more effective if we delve into the unique neural mechanisms underlying emotional dysregulation. Understanding how neural networks contribute to dysregulated emotional responses allows for the development of more personalized treatments, including neurostimulation treatments. As treatments have emerged targeting specific disruptions in emotion regulation networks, a similar approach can be taken to identify unique signatures of emotional dysregulation and target interventions toward these mechanisms. Our preliminary findings provide new avenues that could be explored for transdiagnostic emotional dysregulation interventions. Specifically, the right dlPFC, the left dmPFC, the right OFC, insula-vlPFC connectivity, and insula-dmPFC connectivity are promising targets for neuroscience-driven emotion regulation interventions.

Funding

This research and the completion of the manuscript were supported by a KL2 award granted to the first author by the National Center for Advancing Translational Sciences of the National Institutes of Health under Award Number 5KL2TR001115 and by an NIH R01 award (1R01MH129302-01A1; PI: Neacsiu). Ms. Gerlus was also supported through a T32 award (T32 GM007171; PI: Kontos) and through an F30 aware (F30 MH134460-01A1; PI: Gerlus).

CRediT authorship contribution statement

Andrada D. Neacsiu: Writing – review & editing, Writing – original draft, Supervision, Resources, Project administration, Methodology, Investigation, Funding acquisition, Formal analysis, Data curation, Conceptualization. **Nimesha Gerlus:** Writing – review & editing, Writing – original draft, Formal analysis, Data curation. **John L. Graner:** Writing – review & editing, Writing – original draft, Software, Resources, Formal analysis, Conceptualization. **Lysianne Beynel:** Writing – review & editing, Resources, Methodology, Investigation. **Moria J. Smoski:** Writing – review & editing, Supervision, Methodology, Investigation, Conceptualization. **Kevin S. LaBar:** Writing – review & editing, Supervision, Resources, Methodology, Funding acquisition, Conceptualization.

Declaration of competing interest

The authors reported no biomedical financial interests or potential conflicts of interest.

Supplementary materials

Supplementary material associated with this article can be found, in the online version, at doi:10.1016/j.pscychresns.2024.111891.

References

Bachevalier, J., Loveland, K.A., 2006. The orbitofrontal–amygdala circuit and self-regulation of social–emotional behavior in autism. Neurosci. Biobehavioral Rev. 30 (1), 97–117.

Baumann, O., Mattingley, J.B., 2012. Functional topography of primary emotion processing in the human cerebellum. Neuroimage 61 (4), 805–811.

Benjamini, Y., Hochberg, Y., 1995. Controlling the false discovery rate: a practical and powerful approach to multiple testing. J. Royal Stat. Society: series B (Methodol.) 57 (1), 289–300.

Berboth, S., Morawetz, C., 2021. Amygdala-prefrontal connectivity during emotion regulation: a meta-analysis of psychophysiological interactions. Neuropsychologia 153, 107767.

Bradley, M.M., Sabatinelli, D., Lang, P.J., Fitzsimmons, J.R., King, W., Desai, P., 2003. Activation of the visual cortex in motivated attention. Behav. Neurosci. 117 (2), 369.

Braunstein, L.M., Gross, J.J., Ochsner, K.N., 2017. Explicit and implicit emotion regulation: a multi-level framework. Soc. Cogn. Affect. Neurosci. 12 (10), 1545–1557.

Buhle, J.T., Silvers, J.A., Wager, T.D., Lopez, R., Onyemekwu, C., Kober, H., et al., 2014. Cognitive reappraisal of emotion: a meta-analysis of human neuroimaging studies. Cereb. Cortex. 24 (11), 2981–2990.

Carlén, M., 2017. What constitutes the prefrontal cortex? Science (1979) 358 (6362), 478–482.

Cauda, F., Costa, T., Torta, D.M., Sacco, K., D'Agata, F., Duca, S., et al., 2012. Meta-analytic clustering of the insular cortex: characterizing the meta-analytic connectivity of the insula when involved in active tasks. Neuroimage 62 (1), 343–355.

Cheng, S., Qiu, X., Li, S., Mo, L., Xu, F., Zhang, D., 2022. Different roles of the left and right ventrolateral prefrontal cortex in cognitive reappraisal: an online transcranial magnetic stimulation study. Front. Hum. Neurosci. 16.

Clark, D.A., 2013. Cognitive restructuring. The Wiley handbook of Cognitive Behavioral Therapy, pp. 1–22.

Cooper, S.E., Hennings, A.C., Bibb, S.A., Lewis-Peacock, J.A., Dunsmoor, J.E., 2024. Semantic structures facilitate threat memory integration throughout the medial temporal lobe and medial prefrontal cortex. Curr. Biol. 34 (15), 3522–3536 e5.

De la Peña-Arteaga, V., Berruga-Sánchez, M., Steward, T., Martínez-Zalacaín, I., Goldberg, X., Wainsztein, A., et al., 2021. An fMRI study of cognitive reappraisal in major depressive disorder and borderline personality disorder. Eur. Psychiatry 64 (1), e56.

Dixon, M.L., Thiruchselvam, R., Todd, R., Christoff, K., 2017. Emotion and the prefrontal cortex: an integrative review. Psychol. Bull. 143 (10), 1033.

Doré, B.P., Rodrik, O., Boccagno, C., Hubbard, A., Weber, J., Stanley, B., et al., 2018. Negative autobiographical memory in depression reflects elevated amygdala-hippocampal reactivity and hippocampally associated emotion regulation. Biol. Psychiatry: Cognitive Neurosci. Neuroimaging 3 (4), 358–366.

Dunn, L.M., 1981. PPVT-revised Manual, 1981. American Guidance Service, Circle Pines, MN.

Dörfel, D., Lamke, J.-P., Hummel, F., Wagner, U., Erk, S., Walter, H., 2014. Common and differential neural networks of emotion regulation by detachment, reinterpretation, distraction, and expressive suppression: a comparative fMRI investigation. Neuroimage 101, 298–309.

Esteban, O., Birman, D., Schaer, M., Koyejo, O.O., Poldrack, R.A., Gorgolewski, K.J., 2017. MRIQC: advancing the automatic prediction of image quality in MRI from unseen sites. PLoS. One 12 (9), e0184661.

Esteban, O., Markiewicz, C.J., Blair, R.W., Moodie, C.A., Isik, A.I., Erramuzpe, A., et al., 2019. fMRIPrep: a robust preprocessing pipeline for functional MRI. Nat. Methods 16 (1), 111.

Etkin, A., Büchel, C., Gross, J.J., 2015. The neural bases of emotion regulation. Nature Rev. Neurosci. 16 (11), 693–700.

Fan, L., Li, H., Zhuo, J., Zhang, Y., Wang, J., Chen, L., et al., 2016. The human brainnetome atlas: a new brain atlas based on connectional architecture. Cereb Cortex. 26 (8), 3508–3526.

Feeser, M., Prehn, K., Kazzer, P., Mungee, A., Bajbouj, M., 2014. Transcranial direct current stimulation enhances cognitive control during emotion regulation. Brain Stimul. 7 (1), 105–112.

Fernandez, K.C., Jazaieri, H., Gross, J.J., 2016. Emotion regulation: a transdiagnostic perspective on a new RDoC domain. Cognit. Ther. Res. 40 (3), 426–440.

First, M.B., Williams, J.B., Karg, R.L., 2015. Structured Clinical Interview for DSM-5 Disorders (Research Version: SCID-5-RV). American Psychiatric Publishing, Washington, DC.

Frank, D., Dewitt, M., Hudgens-Haney, M., Schaeffer, D., Ball, B., Schwarz, N., et al., 2014. Emotion regulation: quantitative meta-analysis of functional activation and deactivation. Neurosci. Biobehavioral Rev. 45, 202–211.

Fulwiler, C.E., King, J.A., Zhang, N., 2012. Amygdala-orbitofrontal resting state functional connectivity is associated with trait anger. Neuroreport 23 (10), 606.

Giromini, L., Ales, F., de Campora, G., Zennaro, A., Pignolo, C., 2017. Developing age and gender adjusted normative reference values for the difficulties in emotion regulation scale (DERS). J. Psychopathol. Behav. Assess. 39, 705–714.

Goldin, P.R., McRae, K., Ramel, W., Gross, J.J., 2008. The neural bases of emotion regulation: reappraisal and suppression of negative emotion. Biol. Psychiatry 63 (6), 577–586.

Goldin, P.R., Ziv, M., Jazaieri, H., Werner, K., Kraemer, H., Heimberg, R.G., et al., 2012. Cognitive reappraisal self-efficacy mediates the effects of individual cognitive-behavioral therapy for social anxiety disorder. J. Consult. Clin. Psychol. 80 (6), 1034.

Gratz, K.L., Roemer, L., 2004. Multidimensional assessment of emotion regulation and dysregulation: development, factor structure, and initial validation of the difficulties in emotion regulation scale. J. Psychopathol. Behav. Assess. 26 (1), 41–54.

Greenberg, D.L., Rice, H.J., Cooper, J.J., Cabeza, R., Rubin, D.C., LaBar, K.S., 2005. Co-activation of the amygdala, hippocampus and inferior frontal gyrus during autobiographical memory retrieval. Neuropsychologia 43 (5), 659–674.

Gross, J.J., John, O.P., 2003. Individual differences in two emotion regulation processes: implications for affect, relationships, and well-being. J. Pers. Soc. Psychol. 85 (2), 348–362.

Gross, J.J., 2013. Handbook of Emotion Regulation, Second Edition, 2nd Edition ed. The Guilford Press, New York, p. 669. 2013/12/05/.

Gross, J.J., 2015. Emotion regulation: current status and future prospects. Psychol. Inq. 26 (1), 1–26.

Gruber-Baldini, A.L., Velozo, C., Romero, S., Shulman, L.M., 2017. Validation of the PROMIS® measures of self-efficacy for managing chronic conditions. Qual. Life Res. 26 (7), 1915–1924.

Hawley, L.L., Padesky, C.A., Hollon, S.D., Mancuso, E., Laposa, J.M., Brozina, K., et al., 2017. Cognitive-behavioral therapy for depression using mind over mood: CBT skill use and differential symptom alleviation. Behav. Ther. 48 (1), 29–44.

He, Z., Li, S., Mo, L., Zheng, Z., Li, Y., Li, H., et al., 2023. The VLPFC-engaged voluntary emotion regulation: combined TMS-fMRI evidence for the neural circuit of cognitive reappraisal. J. Neurosci. 43 (34), 6046–6060.

Hendler, T., Rotshtein, P., Hadar, U., 2001. Emotion–perception interplay in the visual cortex:"the eyes follow the heart. Cell. Mol. Neurobiol. 21, 733–752.

Holland, A.C., Kensinger, E.A., 2010. Emotion and autobiographical memory. Phys. Life Rev. 7 (1), 88–131.

Holland, A.C., Kensinger, E.A., 2013. The neural correlates of cognitive reappraisal during emotional autobiographical memory recall. J. Cogn. Neurosci. 25 (1), 87–108.

Hu, H., Li, A., Zhang, L., Liu, C., Shi, L., Peng, X., et al., 2024. Goal-directed attention transforms both working and long-term memory representations in the human parietal cortex. PLoS. Biol. 22 (7), e3002721.

Johnstone T., Walter H. The neural basis of emotion dysregulation. 2014.

Jones, M.S., Zhu, Z., Bajracharya, A., Luor, A., Peelle, J.E., 2022. A multi-dataset evaluation of frame censoring for motion correction in task-based fMRI. Apert. Neuro 2, 1.

Kaczkurkin, A.N., Foa, E.B., 2015. Cognitive-behavioral therapy for anxiety disorders: an update on the empirical evidence. Dialogues. Clin. Neurosci. 17 (3), 337.

Kearney, B.E., Terpou, B.A., Densmore, M., Shaw, S.B., Théberge, J., Jetly, R., et al., 2023. How the body remembers: examining the default mode and sensorimotor networks during moral injury autobiographical memory retrieval in PTSD. Neuroimage: clin. 38, 103426.

Keller, M., Mendoza-Quiñones, R., Cabrera Muñoz, A., Iglesias-Fuster, J., Virués, A.V., Zvyagintsev, M., et al., 2022. Transdiagnostic alterations in neural emotion regulation circuits – neural substrates of cognitive reappraisal in patients with depression and post-traumatic stress disorder. BMC. Psychiatry 22 (1), 173.

Kensinger, E.A., Ford, J.H., 2021. Guiding the emotion in emotional memories: the role of the dorsomedial prefrontal cortex. Curr. Dir. Psychol. Sci. 30 (2), 111–119.

Kjærstad, H.L., de Siqueira Rotenberg, L., Knudsen, G.M., Vinberg, M., Kessing, L.V., Macoveanu, J., et al., 2022. The longitudinal trajectory of emotion regulation and associated neural activity in patients with bipolar disorder: a prospective fMRI study. Acta Psychiatr. Scand. 146 (6), 568–582.

Kohn, N., Eickhoff, S.B., Scheller, M., Laird, A.R., Fox, P.T., Habel, U., 2014. Neural network of cognitive emotion regulation—An ALE meta-analysis and MACM analysis. Neuroimage 87, 345–355.

Kross, E., Davidson, M., Weber, J., Ochsner, K., 2009. Coping with emotions past: the neural bases of regulating affect associated with negative autobiographical memories. Biol. Psychiatry 65 (5), 361–366.

Lee, M.J., Romero, S., Velozo, C.A., Gruber-Baldini, A.L., Shulman, L.M., 2019. Multidimensionality of the PROMIS self-efficacy measure for managing chronic conditions. Qual. Life Res. 28 (6), 1595–1603.

Li, W., Yang, P., Ngetich, R.K., Zhang, J., Jin, Z., Li, L, 2021. Differential involvement of frontoparietal network and insula cortex in emotion regulation. Neuropsychologia 161, 107991.

Li, X., Qin, F., Liu, J., Luo, Q., Zhang, Y., Hu, J., et al., 2022. An insula-based network mediates the relation between rumination and interoceptive sensibility in the healthy population. J. Affect. Disord. 299, 6–11.

Luber, B.M., Davis, S., Bernhardt, E., Neacsiu, A., Kwapil, L., Lisanby, S.H., et al., 2017. Using neuroimaging to individualize TMS treatment for depression: toward a new paradigm for imaging-guided intervention. Neuroimage 148, 1–7.

MacNamara, A., Rabinak, C.A., Kennedy, A.E., Fitzgerald, D.A., Liberzon, I., Stein, M.B., et al., 2016. Emotion regulatory brain function and SSRI treatment in PTSD: neural correlates and predictors of change. Neuropsychopharmacol. 41 (2), 611–618.
McLaren, D.G., Ries, M.L., Xu, G., Johnson, S.C., 2012. A generalized form of context-dependent psychophysiological interactions (gPPI): a comparison to standard approaches. Neuroimage 61 (4), 1277–1286.
Mickley, K.R., Kensinger, E.A., 2008. Emotional valence influences the neural correlates associated with remembering and knowing. Cognitive, Affective, Behavioral Neurosci. 8 (2), 143–152.
Mills, C., D'Mello, S., 2014. On the validity of the autobiographical emotional memory task for emotion induction. PLoS. One 9 (4), e95837.
Morawetz, C., Bode, S., Baudewig, J., Kirilina, E., Heekeren, H.R, 2016. Changes in effective connectivity between dorsal and ventral prefrontal regions moderate emotion regulation. Cereb. Cortex. 26 (5), 1923–1937.
Morawetz, C., Bode, S., Derntl, B., Heekeren, H.R., 2017. The effect of strategies, goals and stimulus material on the neural mechanisms of emotion regulation: a meta-analysis of fMRI studies. Neurosci. Biobehavioral Rev. 72, 111–128.
Neacsiu, A.D., Bohus, M., Linehan, M.M., 2013. Dialectical Behavior Therapy: An Intervention for Emotion Dysregulation. Gross, JJ (Ed) Handbook of Emotion Regulation, 2 ed. The Guilford Press, New York, NY, pp. 491–508.
Neacsiu, A.D., Beynel, L., Powers, J.P., Szabo, S.T., Appelbaum, L.G., Lisanby, S.H., et al., 2021. Enhancing cognitive restructuring with concurrent repetitive transcranial magnetic stimulation: a transdiagnostic randomized controlled trial. PsychOther Psychosom.
Neacsiu, A.D., Beynel, L., Graner, J.L., Szabo, S.T., Appelbaum, L.G., Smoski, M.J., et al., 2022. Enhancing cognitive restructuring with concurrent fMRI-guided Neurostimulation for Emotional Dysregulation: a randomized controlled trial. J. Affect. Disord. 301, 378–389.
Nieto-Castañón, A., Fedorenko, E., 2012. Subject-specific functional localizers increase sensitivity and functional resolution of multi-subject analyses. Neuroimage 63 (3), 1646–1669.
Nolen-Hoeksema, S., 2012. Emotion regulation and psychopathology: the role of gender. Annu Rev. Clin. Psychol. 8 (1), 161–187.
O'Reilly, J.X., Woolrich, M.W., Behrens, T.E., Smith, S.M., Johansen-Berg, H., 2012. Tools of the trade: psychophysiological interactions and functional connectivity. Soc. Cogn. Affect. Neurosci. 7 (5), 604–609.
Ochsner, K.N., Silvers, J.A., Buhle, J.T., 2012. Functional imaging studies of emotion regulation: a synthetic review and evolving model of the cognitive control of emotion. Ann. N. Y. Acad. Sci. 1251, E1–24.
Peer, M., Abboud, S., Hertz, U., Amedi, A., Arzy, S., 2016. Intensity-based masking: a tool to improve functional connectivity results of resting-state fMRI. Hum. Brain Mapp. 37 (7), 2407–2418.
Pico-Perez, M., Radua, J., Steward, T., Menchon, J.M., Soriano-Mas, C., 2017. Emotion regulation in mood and anxiety disorders: a meta-analysis of fMRI cognitive reappraisal studies. Prog. Neuropsychopharmacol. Biol. Psychiatry 79 (Pt B), 96–104.
Power, J.D., Barnes, K.A., Snyder, A.Z., Schlaggar, B.L., Petersen, S.E., 2012. Spurious but systematic correlations in functional connectivity MRI networks arise from subject motion. Neuroimage 59 (3), 2142–2154.
Power, J.D., Mitra, A., Laumann, T.O., Snyder, A.Z., Schlaggar, B.L., Petersen, S.E., 2014. Methods to detect, characterize, and remove motion artifact in resting state fMRI. Neuroimage 84, 320–341.
Powers, J.P., LaBar, K.S., 2019. Regulating emotion through distancing: a taxonomy, neurocognitive model, and supporting meta-analysis. Neurosci. Biobehav. Rev. 96, 155–173.
Powers, J.P., Graner, J.L., LaBar, K.S., 2019. Multivariate patterns of posterior cortical activity differentiate forms of emotional distancing. Cerebral cortex.
Rolls, E.T., Deco, G., Huang, C.-C., Feng, J., 2023. Human amygdala compared to orbitofrontal cortex connectivity, and emotion. Prog. Neurobiol. 220, 102385.
Schutter, D.J., Van Honk, J., 2005. A framework for targeting alternative brain regions with repetitive transcranial magnetic stimulation in the treatment of depression. J. Psychiatry Neurosci. 30 (2), 91–97.
Siegel, J.S., Power, J.D., Dubis, J.W., Vogel, A.C., Church, J.A., Schlaggar, B.L., et al., 2014. Statistical improvements in functional magnetic resonance imaging analyses produced by censoring high-motion data points. Hum. Brain Mapp. 35 (5), 1981–1996.
Silvers, J., Buhle, J.T., Ochsner, K.N., 2013. The Neuroscience of Emotion Regulation. The Oxford Handbook of Cognitive Neuroscience.
Skodol, A.E., Bender, D.S., 2003. Why are women diagnosed borderline more than men? Psychiatr. Q. 74, 349–360.
Smoski, M., Diehl, J., Graner, J., Madden, D., Erkanli, A., LaBar, K., 2024. Neurocognitive predictors of emotion regulation success in mid-to late-life depression. Am. J. Geriatric Psychiatry 32 (4), S100–S1S1.
Sonkusare, S., Qiong, D., Zhao, Y., Liu, W., Yang, R., Mandali, A., et al., 2022. 39 Frequency Dependent Emotion Differentiation and Directional Coupling in amygdala, Orbitofrontal and Medial Prefrontal Cortex Network With Intracranial Recordings. BMJ Publishing Group Ltd.
Stephanou, K., Davey, C.G., Kerestes, R., Whittle, S., Harrison, B.J., 2017. Hard to look on the bright side: neural correlates of impaired emotion regulation in depressed youth. Soc. Cogn. Affect. Neurosci. 12 (7), 1138–1148.
Suzuki, Y., Tanaka, S.C., 2021. Functions of the ventromedial prefrontal cortex in emotion regulation under stress. Sci. Rep. 11 (1), 18225.
Talarico, J.M., LaBar, K.S., Rubin, D.C., 2004. Emotional intensity predicts autobiographical memory experience. Mem. Cognit. 32 (7), 1118–1132.
Taylor, S.F., Liberzon, I., 2007. Neural correlates of emotion regulation in psychopathology. Trends. Cogn. Sci. 11 (10), 413–418.
Tong, Y., Chen, Q., Nichols, T.E., Rasetti, R., Callicott, J.H., Berman, K.F., et al., 2016. Seeking optimal region-of-interest (ROI) single-value summary measures for fMRI studies in imaging genetics. PLoS. One 11 (3), e0151391.
Tozzi, L., Zhang, X., Pines, A., Olmsted, A.M., Zhai, E.S., Anene, E.T., et al., 2024. Personalized brain circuit scores identify clinically distinct biotypes in depression and anxiety. Nat. Med. 1–12.
Versace, A., Thompson, W.K., Zhou, D., Almeida, J.R., Hassel, S., Klein, C.R., et al., 2010. Abnormal left and right amygdala-orbitofrontal cortical functional connectivity to emotional faces: state versus trait vulnerability markers of depression in bipolar disorder. Biol. Psychiatry 67 (5), 422–431.
Wager, T.D., Davidson, M.L., Hughes, B.L., Lindquist, M.A., Ochsner, K.N., 2008. Neural mechanisms of emotion regulation: evidence for two independent prefrontal-subcortical pathways. Neuron 59 (6), 1037.
Wang, Y., Leung, F., Zhong, J., 2008. The adaptation of McLean screening instrument for borderline personality disorder among Chinese college students. Chinese J. Clin. Psychol. 16 (3), 258–260.
Webb, T.L., Miles, E., Sheeran, P., 2012. Dealing with feeling: a meta-analysis of the effectiveness of strategies derived from the process model of emotion regulation. Psychol. Bull. 138 (4), 775–808.
Wolpe, J., 1969. Subjective units of distress scale. J. EMDR Pract. Res.
Woolrich, M.W., Ripley, B.D., Brady, M., Smith, S.M., 2001. Temporal autocorrelation in univariate linear modeling of FMRI data. Neuroimage 14 (6), 1370–1386.
Woolrich, M.W., Behrens, T.E., Beckmann, C.F., Jenkinson, M., Smith, S.M., 2004. Multilevel linear modelling for FMRI group analysis using Bayesian inference. Neuroimage 21 (4), 1732–1747.
Zaki, J., Davis, J.I., Ochsner, K.N., 2012. Overlapping activity in anterior insula during interoception and emotional experience. Neuroimage 62 (1), 493–499.
Zilverstand, A., Parvaz, M.A., Goldstein, R.Z., 2017. Neuroimaging cognitive reappraisal in clinical populations to define neural targets for enhancing emotion regulation. A systematic review. Neuroimage 151, 105–116.